Materials Today Communications 35 (2023) 106300

Contents lists available at ScienceDirect

Materials Today Communications

journal homepage: www.elsevier.com/locate/mtcomm

Stereoselective 1,2 migration of a boronate complex inside a nanoreactor: QM/MM study

Zied Hosni [a,*], Sarra Darghouthi [b], Sofiene Achour [b]

[a] Institute for Materials Discovery, University College London, 40 Roberts Building, London, WC1E 7 JE, United Kingdom
[b] Research Unity of Modeling in Fundamental Sciences and Didactics, University of Tunis El Manar, BP 254, El Manar 2, 2096, Tunisia

ARTICLE INFO

Keywords:
DFT
Carbon nanotube
Reaction confinement
Nanocomposites
Stereoselective reactions

ABSTRACT

In this study, we investigate the stereoselective 1,2 migration reaction inside a carbon nanotube (CNT) using a combined quantum mechanics/molecular mechanics (QM/MM) approach. The steric and electronic effects of the CNT are found to significantly influence the stabilization of the guest molecule, highlighting the importance of nanotube diameter. By adjusting the nanotube diameter, it becomes possible to control the stereoselectivity of the migration reaction. Nanoreactors, such as CNTs, have emerged as promising tools for manipulating chemical reactions due to their versatile properties. We explore the impact of the nanotube environment on the migration mechanism and discuss the role of non-covalent interactions, such as van der Waals forces, in promoting stability and selectivity. Our computational results demonstrate that the presence of the CNT affects the reaction kinetics, energy barriers, and overall energetic outcomes. The choice of nanotube diameter is crucial to achieve optimal confinement of the guest molecule while maintaining stabilizing interactions. This study provides valuable insights into the potential of carbon nanotubes as nanoreactors for controlling stereochemistry in organic reactions, offering opportunities for tailored reaction design and synthesis.

Nanoreactors have become, during the last decades, a novel approach to conduct physical or chemical manipulation such as drugs carrier, or energy storage, or water purification [1]. Carbon is crucial due to its versatile properties. Recent research has showcased the broad applicability of nanostructures and nanocomposites in fields such as photocatalysis, environmental remediation, and even potential hydrogen storage [2–5]. Recently, carbon nanotubes have been utilized to manipulate reaction energy surfaces, allowing for precise control of chemical reaction reactivity. The inherent and tuneable geometry constraint inside the nanotube enables the control of reactions rate and thermodynamic properties [6]. The orientation of the small molecule within the tube consequently affects the regioselectivity of the reaction of interest [7]. Non-covalent bonds such as van der Waals interactions promote the stabilisation of the environment between the endohedral system and the electron cloud of the surrounding CNT [8]. The estimation of the adsorption energy inside the CNT showed this process can be exothermic or endothermic according to the internal van der Waals diameter of the nanotube [9]. Encapsulation influences activity, stability, and selectivity [10]. Organ boranes and boronic esters present an important class of compounds exploited as synthetic intermediates in various reactions and susceptible to be convert into various functional groups with optimum stereospecificity. The initial nucleophilic addition of an organolithium to an electrophilic boron atom results in the formation of a tetracoordinate 'ate' complex, followed by 1,2 migration.

The appropriate nanotube diameter was determined through testing different sizes and measuring the confinement energy using equation (Eq. 1). Thus, the nanotube that provides the lowest confinement energy is the most suitable to simulate the stereoselective reaction. Initially, the guest molecule was optimized within various carbon nanotubes, and then, a single point calculation was performed separately on the guest and host without modifying their structures further.

$$E_{confinment} = E_{guest@CNT} - E_{Free,CNT} - E_{free,Guest} \quad (1)$$

To achieve satisfactory convergence, ultrafine integration grids and tight convergence criteria were employed. After an initial optimization in the gas phase, a corrective solvent continuum model (SMD) was used with a final single point at the same level of theory to include the effect of bulk solvent (Et2O) [11]. All studied systems were treated with DFT calculations using the M06–2X functional [12]. The latter has been considered as a QM reference as it has proven to show good agreement with experimental results in many computational problems and

* Corresponding author.
E-mail address: zyedhosny@gmail.com (Z. Hosni).

https://doi.org/10.1016/j.mtcomm.2023.106300
Received 10 April 2023; Received in revised form 22 May 2023; Accepted 23 May 2023
Available online 2 June 2023

especially in cases of small molecules confined inside carbon nanotube where it is vital to treat the non-covalent interaction between the internal wall of the tube and the electronic cloud of the guest molecule. Reducing the CNT volume results in an asymptotic increase of the energy of the considered molecule due to the structural distortion of the transition state. An excessive increase of the CNT diameter leads to the loss of stabilizing energy from the C−H···π interactions [13]. The UFF force field considers only van der Waals interactions (in the Lennard-Jones-type form) [14]. ONIOM calculations produce a good compromise between precision and computational cost especially when studying systems with hundreds of atoms and the accurate energy calculation is necessary to accurately describe the reactivity [15]. The carbon nanotube was always placed into the low layer and treated using the molecular mechanics (MM) level of theory using the universal force field (UFF). This force field explains properly the system in terms of noncovalent interactions (van der Waals) between the endohedral system and the electronic cloud of the surrounding CNT [16]. Hydrogen atoms were added to the open ends of the CNTs to avoid dangling bonds considering mechanical and electrostatic embedding [17]. Harmonic vibrational frequencies were computed to confirm the stable configurations and transition states by identifying a single imaginary frequency for TSs and no imaginary frequencies in ground-state structures. The inner layer (high-level layer) consists of of the boronate-carbamate complex and the outer layer (low-level layer) consists of the carbon nanotube. All calculations were performed using a Gaussian 03 program package [18].

The 1,2 migration in boronate complex can follow two distinctive pathways (the concerted and the stepwise pathway as illustrated in Fig. 1) and can involve two different centres (the methyl group or one of the oxygens on the boron). When the concerted pathway is considered, the migration follows an SN2-type mechanism where the migrating group moves from the boron to the adjacent methylene with simultaneous cleavage of the carbamate. When the stepwise pathway is considered, the boronate complex undergoes an initial cleavage of the carbamate and the formation of a carbocation as a result of an SN1-type reaction, followed by the migration of the methyl or the oxygen toward the neighbouring carbon.

Before investigating the reaction mechanism of migration, we scanned the dihedral angle between the atoms involved in the migration process. Indeed, the scan of the dihedral angle C1-B-C2-O2 indicated that the reagent needs to be activated to be ready for the migration of C or O. When the torsion is plane then the C1 and O2 are o an anti-periplanar position that enables the migration of the methyl group from the boron to the carbon in the alpha position. A rotation with 60° of the same dihedral angle puts the O1 in the anti-periplanar position, which activates the molecule for the O migration (i.e. the dihedral angle O1-B-C2-O2 is −180 C). The homologue scan of the same dihedral angle within the carbon nanotube rendered the same result. The choice of this diameter for the carbon nanotube depends on the interaction between the host and the guest molecule.

The selection of a nanotube with an excessively large diameter would push the guest outside the nanocarrier and it would not be able to confine it. Similarly, the choice of a nanotube with a too-narrow diameter would not allow the penetration of the boron molecule inside the tube [19]. The most suitable diameter of the nanotube is providing enough space for the guest to enter inside it while also, it is mutually stabilising the host through non-covalent bonds such as van der Waals interactions. In other terms, the nanotube is behaving like a "nanoglu" to retain the guest within the internal wall of the CNT as shown in Fig. 2. We tested nanotubes with diameters ranging from (5,5) to (11,11), corresponding to a diameter between 6.5 Å and 15.5 Å. The carbon nanotube with a diameter of 9.6 Å, corresponding to (7,7), exhibited the lowest confinement energy.

The choice of the minimum nanotube width automatically depends on the dimensions of the largest species along the reaction pathway. The diffusion of the reactant into the inner cavity of the CNT is modulated

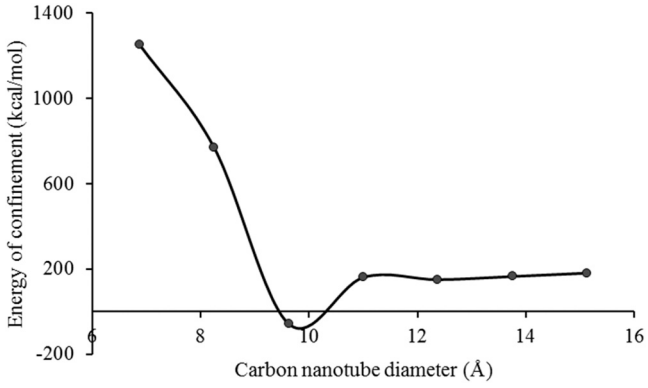

Fig. 2. Variation of the interaction energy versus CNT's diameter.

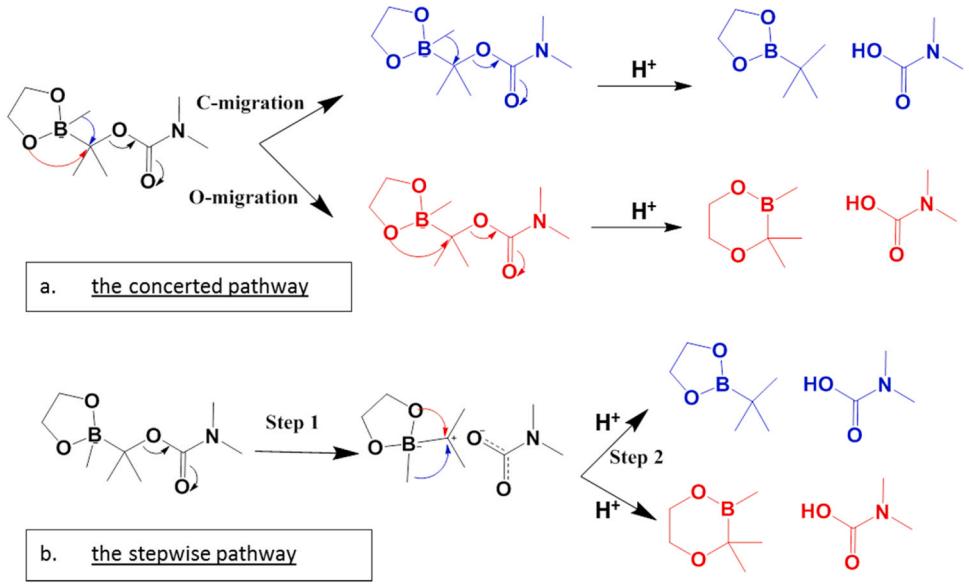

Fig. 1. The two pathways (a and b) of the C-migration in blue and O- migration in red in boronate complexes.

through the noncovalent bond between the boronic ester molecule and the π-framework built by the interior of the nanotube. The regioselectivity of the reaction is determined by the flexibility of the reactants. A specific regioisomer is energetically more favourable by a conformational rearrangement of the transition state induced by the steric constraint within the CNT cavity as depicted in Fig. 3. The steric and electronic effects balance have a complementary impact on the effectiveness of confinement inside the CNT and the selectivity modulation without a catalyst [20]. Spatial restriction influences the adsorption activation of reactants and hence the catalytic activity. CNT surface can modify the diffusion behaviour and result in the enrichment of reactants inside the CNT channels, which provides additional opportunities to modulate the catalytic performance [21].

Lower barrier and lower endothermicity can be attributed to a complex interplay between C—H···π, N – H···π, and Cl···π nonbonded interactions of the endohedral system with the electron cloud of the CNT wall [22]. This migration reaction has been previously investigated in numerous computational studies, involving different migrating groups, leaving groups, or substituents at boron [23]. The mechanism of migration between boron and carbon atoms can be explained by a clear SN2-like trigonal bipyramidal arrangement of groups around the latter. The activation barrier for C-migration following the concerted path is 30.65 kcal/mol, as shown in Fig. 4, which is 6.35 kcal/mol more favorable than O-migration. The thermodynamic stability of the C-migration product is higher than that of the O-migration product, with a corresponding energy of reaction of − 27.006 kcal/mol. A catalyst is required to lower this high activation barrier. Utilizing CNT to facilitate the 1,2 migration results in a product with lower energy compared to the case without the nanotube. For example, the potential energies of the C and O migration products are − 59.57 and 12.96 kcal/mol, respectively, compared to − 27.006 and 10.748 kcal/mol in the absence of CNT. In the stepwise path of the 1,2 migration, the release of the carbamate group and the formation of the carbocation constitute the kinetically limiting step, following an SN1 mechanism.

The activation energies for TS1 are 25.69 and 27.33 kcal/mol for C and O migration, respectively. The second step has a lower activation barrier with energies of 5.36 and − 17.30 kcal/mol for C and O migration, respectively. The product of C migration, when the CNT is excluded, is 37.75 kcal/mol lower than in the case of O-migration, indicating its thermodynamic favorability. When the 1,2 migration is carried out inside the CNT, the release of the carboxylated group becomes the kinetically determining step.

Thus, the activation barriers for releasing the carbamate group are 24.83 and 33.43 kcal/mol for C and O migration, respectively, compared to 23.44 kcal/mol for the direct pathway. The product of C migration in the CNT is thermodynamically more favorable, with a potential energy of − 59.57 kcal/mol compared to 12.96 kcal/mol for O migration. It is important to note that O-migration is not spontaneous in the direct pathway. In the case of the stepwise pathway without the CNT, C-migration is kinetically more favorable, with an activation barrier 6.68 kcal/mol lower than O-migration in the solvent. Inside the CNT, the stepwise path favors O-migration, as its activation barrier is 5 kcal/mol compared to C-migration, as shown in Fig. 5.

The introduction of the CNT stabilizes the intermediate of the reaction in the stepwise pathway, resulting in a decrease in its potential energy. The nanotube achieves this by establishing non-covalent interactions between the π-bond of the CNT network and the hydrogen of both the boron compound and the leaving group. The stabilization of the intermediate and the corresponding transition state towards the product is more pronounced inside the CNT, with the energy of TS2 being 8 kcal/mol lower.

During the concerted migration of the pinacol oxygen, the carbamate moiety was simultaneously released. In the transition state, the C2-O2 bond was broken, resulting in an increase in the C2-O2 distance by 1.1 Å, which continued to move away from the initial reagent until reaching 4.67 Å.

The methyl group attached to the boron atom remained unchanged during the reaction. Surprisingly, the bond C2-O1 was slightly longer during the transition state than when the bond was formed, and the distance reached 1.433 Å. To facilitate the O-migration, the dihedral angle O1-B-C2-O2 was nearly planar, creating an activated complex capable of undergoing O migration. As the oxygen migrated away from the boron, the Mulliken charge of the boron decreased by 0.06 C. The release of the carbamate group reduced the withdrawal of electronic charge caused by C2.

In the concerted pathway of the C-migration reaction in the SMD model of an ether solvent, the distance C2-O2 extended by 5 Å, indicating the release of the carbamate group. The negative charge of oxygen O2 increased from − 0.319 C to − 0.604 C at the product, explaining the complete liberation of the carbamate group. In the reagent stage, when the migrating methyl was on the poorly charged boron, the charge of C1 was − 0.663, and then reduced to − 0.421 C at the product. The concerted migration of the methyl group occurred when the reagent was activated by a free rotation of the σ-bond between B and C1. The dihedral angle C1-B-C2-O2 was 170.06° at the activated complex of the reagent, and then slightly expanded to 174.92° at the transition state. This pathway demonstrates a nucleophilic substitution SN2.

In the O-migration pathway in the same SMD model, the 5-membered ring expanded to a 6-membered ring. As a result, the bond O1-B was cleaved, and the bond O2-C2 was formed. The distance B-O1 increased by 0.9 Å, while the distance O1-C2 decreased by 1.1 Å. This

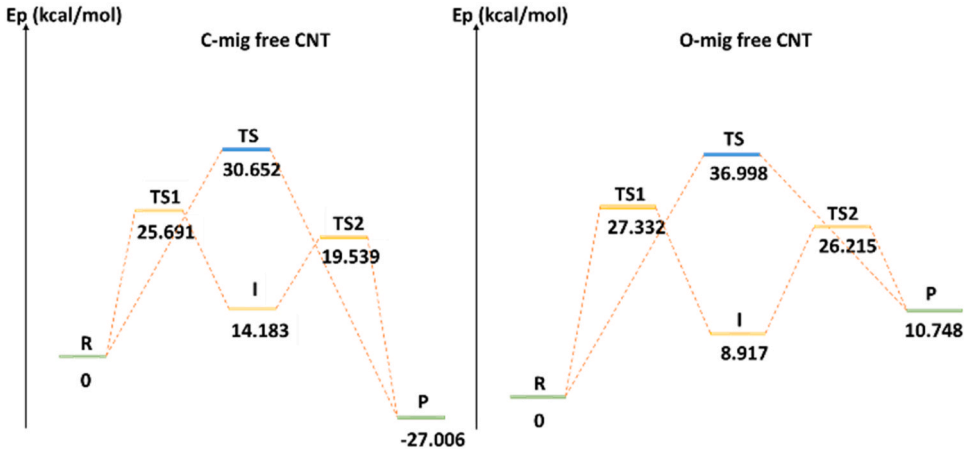

Fig. 3. The energetic profiles of the 1,2 migration of the oxygen or the carbon following the concerted and the stepwise pathways in a SMD model.

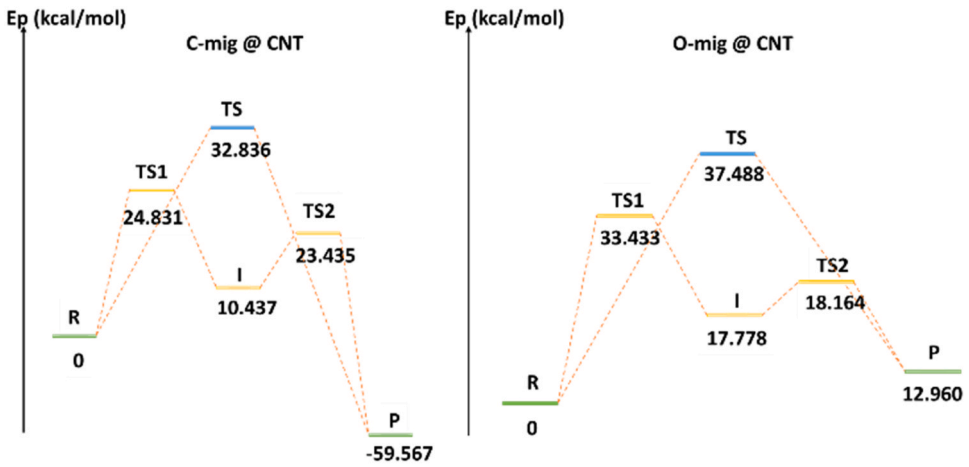

Fig. 4. The energetic profiles of the 1,2 migration of the oxygen or the carbon following the concerted and the stepwise pathways within a (7,7) carbon nanotube.

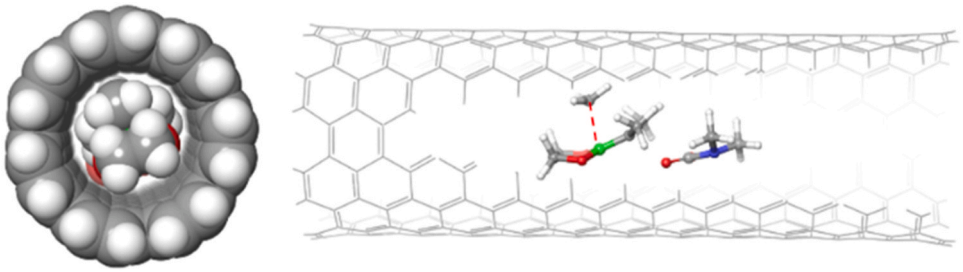

Fig. 5. Front (on the left) and lateral (on the right) views of the confined boronate complex within an uncapped carbon nanotube.

oxygen migration was activated by the positioning of the atom in an anti-periplanar configuration relative to the O2 of the carbamate.

During the migration, the boron lost a significant portion of its electronic density, as it was withdrawn by two oxygens in the reagent stage and by a single oxygen at the product stage. This is illustrated by a more pronounced loss of positive charge on the boron (0.385 C at the product of the C-migration vs. 0.288 C at the O-migration). The confinement of the product inside the carbon nanotube did not alter the geometry. Additionally, the negatively charged carbamate that was cleaved from the boron complex remained stable, and the nanotube did not expel it. The oxygen of the carbamate was stabilized by the neighboring hydrogens of the pinacol group.

We designed the two migration pathways while adhering to the experimental conditions [24]. Therefore, we employed the SMD (Solvation Model based on Density) model with diethyl ether as a non-polar solvent.

We expect that the steric effects would be omitted in this case. The stabilisation of the carbamate inside the nanotube was more accentuated as we noticed that the convergence of the optimisation was reached when the leaving group was farther in the case of the reaction in the SMD model. Thus, the distance C2-O2 was 4.674 Å and 3.919 Å in the nanotube and in the solvent, respectively. The dipole moment in the CNT was 10.21 Debye which is almost double the one in SMD with an axis parallel to the axis of the nanotube in both cases. This confirms that the release of the carbamate was inherently facilitated by the presence of the nanotube. The steric effects contributed slightly to the conformation of the O-migration product as the cleaved bond B-O1 was 2.541 Å in SMD against 2.387 Å in CNT. Besides, the steric effects contributed to a planar dihedral angle where the migration occurred. Indeed, this torsion was 179°, 168° in SMD and CNT, respectively.

By comparing the release of the carbamate in the case of SMD and within the CNT, one notices that the obtained intermediate has a slightly different geometry. Thus, the distance C2-O2 was 0.2 Å larger when the nanotube was not considered w, which could be explained by the absence of the steric hindrance in SMD. The dihedral angle between the migrating group and the leaving group at the transition state that follows the formation of the intermediate shows an activated complex where the torsion was equal to 160° in both cases (i.e. in SMD and in CNT). The charge of C2 was 0.03 C higher when the carbon nanotube encapsulated the boron complex. The case of the O-migration followed an SN1 mechanism. The first step of the stepwise pathway (i.e. the cleavage of the carbamate) was characterised by a more pronounced distance between the leaving oxygen of the carbamate and C2, which is the carbon receiving the migrating methyl group. Therefore, this distance in the intermediate confined in the CNT was 0.21 Å longer than the case of SMD model. At this step, the charge of C2 was 0.16 C lower in the case of SMD. The formation of the intermediate translates to the presence of a carbocation, which was more stabilised in the carbon nature (i.e. its Mulliken charge was null).

The fundamental changes in the structural properties of the guest species constitute the ground for an in-depth systematic stereochemical investigation of a large variety of compounds inside nanotubes. The results suggest that the impact of the nanotubes on the mechanism of the reaction depends on the diameter of the nanotube. A suitable diameter affect the reaction noticeably. Most of the reactions taking place inside small nanotubes are considerably altered due to the steric hindrance. The presence of the CNT may affect the geometries of the reactants, the reaction energy barriers, as well as the energetic outcome of the reactions. This confirms the potential of the carbon nanotube to adjust the kinetics and the thermodynamics properties of the reaction of interest if we expect a sensitive stereoselectivity to the steric and electronic effect of its environment.

CRediT authorship contribution statement

Zied Hosni: Conceptualization, Methodology, DFT calculation **Sarra**

Darghouthi: Visualization, Investigation Writing – review & editing. **Sofiene Achour**: Data curation, Writing – original draft preparation.

Declaration of Competing Interest

The authors declare that they have no known competing financial interests or personal relationships that could have appeared to influence the work reported in this paper.

Data Availability

Data will be made available on request.

References

[1] Y. Liu, J. Wang, M. Zhang, H. Li, Z. Lin, ACS Nano 14 (2020) 12491–12521.
[2] M.A. Mahdi, S.R. Yousefi, L.S. Jasim, M. Salavati-Niasari, Int. J. Hydrog. Energy 47 (2022) 14319–14330.
[3] S.R. Yousefi, H.A. Alshamsi, O. Amiri, M. Salavati-Niasari, J. Mol. Liq. 337 (2021), 116405.
[4] S.R. Yousefi, M. Masjedi-Arani, M.S. Morassaei, M. Salavati-Niasari, H. Moayedi, Int. J. Hydrog. Energy 44 (2019) 24005–24016.
[5] P. Mehdizadeh, M. Jamdar, M.A. Mahdi, W.K. Abdulsahib, L.S. Jasim, S.R. Yousefi, M. Salavati-Niasari, Arab. J. Chem. 16 (2023), 104579.
[6] U.H.H. Brinker, J.-L. Mieusset, Molecular encapsulation. Wiley Online Library, John Wiley & Sons, 2010.
[7] S.A. Miners, G.A. Rance, A.N. Khlobystov, Chem. Soc. Rev. 45 (2016) 4727–4746.
[8] T.D. Marforio, A. Bottoni, P. Giacinto, F. Zerbetto, M. Calvaresi, J. Phys. Chem. C 121 (2017) 27674–27682.
[9] L. Wang, J. Wu, C. Yi, H. Zou, H. Gan, S. Li, Comput. Theor. Chem. 982 (2012) 66–73.
[10] D. Iglesias, M. Melchionna, Catalysts 9 (2019) 128.
[11] S. Essafi, S. Tomasi, V.K. Aggarwal, J.N. Harvey, J. Org. Chem. 79 (2014) 12148–12158.
[12] Y. Zhao, D.G. Truhlar, Theor. Chem. Acc. 120 (2008) 215–241.
[13] P. Giacinto, A. Bottoni, M. Calvaresi, F. Zerbetto, J. Phys. Chem. C 118 (2014) 5032–5040.
[14] T. Vreven, K. Morokuma, Ö. Farkas, H.B. Schlegel, M.J. Frisch, J. Comput. Chem. 24 (2003) 760–769.
[15] L. Wang, C. Yi, H. Zou, J. Xu, W. Xu, Mater. Chem. Phys. 127 (2011) 232–238.
[16] M.D. Prasanna, T.N. Guru Row, Cryst. Eng. 3 (2000) 135–154.
[17] M.J. Frisch, G.W. Trucks, H.B. Schlegel, et al., G09, Gaussian 09 (Revision D.2), Gaussian, Inc., Pittsburgh, PA., 2009.
[18] R. Bessrour, Y. Belmiloud, Z. Hosni, B. Tangour, AIP Conf. Proc. 1456 (2012) 229–239.
[19] Z. Hosni, R. Bessrour, B. Tangour, J. Comput. Theor. Nanosci. 11 (2014) 318–323.
[20] S.A. Miners, M.W. Fay, M. Baldoni, E. Besley, A.N. Khlobystov, G.A. Rance, J. Phys. Chem. C 123 (2019) 6294–6302.
[21] X. Pan, X. Bao, Acc. Chem. Res. 44 (2011) 553–562.
[22] P. Giacinto, F. Zerbetto, A. Bottoni, M. Calvaresi, J. Chem. Theory Comput. 12 (2016) 4082–4092.
[23] S. Roesner, C.A. Brown, M. Mohiti, A.P. Pulis, R. Rasappan, D.J. Blair, S. Essafi, D. Leonori, V.K. Aggarwal, Chem. Commun. 50 (2014) 4053–4055.
[24] H. Wang, C. Jing, A. Noble, V.K. Aggarwal, Angew. Chem. - Int. Ed. 59 (2020) 16859–16872.